Desalination and Water Treatment
www.deswater.com
doi: 10.1080/19443994.2015.1089197

57 (2016) 18425–18437
August

Taylor & Francis
Taylor & Francis Group

Synthesis of 8-Hydroxyquinoline-functionalized polyglycidy methacrylate resin and its efficient adsorption and desorption for Pb(II)

Chunping Liu[a,*], Xiaoli Sun[b], Lin Liu[b], Junshen Liu[a], Minyi Qi[a], He An[a]

[a]*School of Chemistry and Materials Science, Ludong University, Yantai 264025, China, Tel. +86 535 6672609; Fax: +86 535 6696162; emails: chemlcp@sina.com (C.P. Liu), liujunshen@163.com (J.S. Liu), 499385773@qq.com (M.Y. Qi), 306351660@qq.com (H. An)*

[b]*Wanhua Chemical Group Co. Ltd, Yantai 264002, China, Tel./Fax: +86 535 8202637; email: sxly28@163.com (X.L. Sun), liulin@whchem.com (L. Liu)*

Received 27 January 2015; Accepted 27 August 2015

ABSTRACT

The adsorbent 8-hydroxyquinoline-modified PGMA (HQPGMA resin) was synthesized via "graft from" method. The adsorption and desorption performances for Pb(II) were investigated in detail. The maximum uptake was determined at 1.38 mmol g^{-1} with an initial concentration of Pb(II) 0.02264 mol L^{-1}, pH 5.81, and temperature 25°C. The equilibrium time of adsorption kinetics for Pb(II) was 600 min. The adsorption process conformed to pseudo-second-order model. Film diffusion was the rate-limit step. Freundlich model fits the adsorption isothermal process. The thermodynamic parameters implied the adsorption was exothermic and spontaneous. Pb(II) adsorbed on the resin can be eluted by a range of concentrations of hydrochloric acid from 0.2 to 0.8 mol L^{-1} solution. The optimal concentration of hydrochloric acid solution was achieved with 0.4 mol L^{-1}, which resulted in a desorption rate of 92.38%. The resin demonstrated reusability with same effect after three times of adsorption/desorption cycles.

Keywords: 8-Hydroxyquinoline; Graft from; HQPGMA resin; Adsorption; Desorption; Pb(II)

1. Introduction

Clean water shortage becomes a global concern, and heavy metals such as lead, mercury, cadmium are major pollutants [1,2]. Numerous studies showed that heavy metals endanger both natural environments and human health [3,4]. Among all heavy metals, lead(II), (Pb(II)), becomes a serious concern for human health because of its bioavailability and high toxicity for neural systems. Lead contamination was introduced mostly by industry such as mining, battery manufacturing, and pesticides [5–8]. The guideline for maximum concentration of Pb(II) in drinking water is now 0.01 mg L^{-1} [9]. The toxicity of Pb(II) is caused by its high affinity for bindings of important enzymes, and leads to loss of cell functions. The exposure to excessive levels of Pb(II) is associated with multiple human diseases such as finger tremor, radius nerve palsy [10]. Therefore, it is extremely urgent to control Pb(II) below the limit by the elimination of Pb(II) from water sources such as sewage.

Some common approaches to remove Pb(II) from wastewater include chemical deposition [11], electrolytic process [12], ion exchange method [13], and

*Corresponding author.

adsorption method [14]. While chemical deposition and ion exchange have limitation in cost, feasibility and may cause environment problem, adsorption is considered as one of the most promising methods. The advantages of this approach include the following: low cost, high efficiency, reversibility, and easiness to set up [15,16]. Success application of this technique is dependent on appropriate adsorbents, which determined the loading capacities of Pb(II).

Generally, the adsorbents are classified into four categories according to their chemical structure. They are carbon adsorbent materials [17], inorganic adsorbent materials [18], polymer adsorbent materials [19], and biological adsorbent materials [20]. Among these adsorbents, a type of polymer adsorbent material, named synthetic resin, receives increasing attention [21–23]. Chelating resins, as one of the most popular synthetic polymers, are promising in the removal of metal ions because they have advantages of high loading capacity, easiness in handling, reusability, and low cost [24]. It has been reported that adsorbents with the functional groups such as carboxyl, sulfonic, and phosphonic have high affinity for metal ions through the ion exchange mechanism, while those containing nitrogen facilitate metal ions adsorption via chelation mechanism [25,26]. In general, "graft from," "graft to," and "graft through" are the commonly used methods to synthesize macromolecular skeleton-functional group conjugates, of which "graft from" distinguished itself due to inherent higher conjugation efficiency and easier purification.

8-Hydroxyquinoline (8-HQ) can coordinate with metal ions from the stable chelating complex with its bidentate ligand [27]. It is frequently used as solvent extraction agent and metal ion precipitating agent [28]. However, its application is limited because it has high solubility in alkaline or acid solution. Hence "graft from" technique as highly efficient means to solve this issue. The adsorbents based on this method have good chelating properties with adequately available nitrogen groups; moreover, it possesses high mechanical strength and can be reused.

In this work, we chose spherical polyglycidyl methacrylate (PGMA) to build the macromolecular skeleton because it has high specific surface area. The final adsorbent 8-HQ-functionalized PGMA resin (HQPGMA) was synthesized via "graft from" method with diethylenetriamine (DETA) as bridge agent, and 5-chloromethylation-8-HQ as the functional group. The adsorption properties for Pb(II) in terms of befitting pH, contact time, and temperatures were evaluated comprehensively. Desorption properties of HQPGMA resin with different concentrations of hydrochloric acid solution were also determined.

2. Materials and methods

2.1. Materials

Glycidyl methacrylate (GMA) (Shanghai Shijin Chemical Co., Shanghai, China) was purified via vacuum distillation prior to being preserved at 5℃. Divinyl benzene (DVB) (A.R. grade, Tianjin Damao Chemical Co., Tianjin, China) was dealt with lye and dried before used. 2,2′-Azodiisobutyronitrile (AIBN) (A.R. grade, Tianjin Fuchen Chemical Reagent Co., Tianjin, China) was further purified by recrystallization. 8-HQ (>99.5%, Tianjin Damao Chemical Co., Tianjin, China), diethylenetriamine (DETA) (98.0%, Jinan Aoxing Chemical Co., Jinan, China), ethylenediamine tetraacetic acid (EDTA) (>99%, Jiangsu Yixing Chemical Regent Co., Jiangsu, China), methanol (A.R. grade, Tianjin Damao Chemical Reagent Co., Tianjin, China), ethyl alcohol (A.R. grade, Laiyang Economic and Technological Development Zone Fine Chemical Co., Yantai, China), 1,4-dioxane (Shanghai Huyu Biological Technology Co., Shanghai, China), and sodium bicarbonate ($NaHCO_3$) (A.R. grade, Guoyao Group Chemical Reagent Co., Beijing, China) were used without purification. All other chemicals were used as received unless specially indicated.

2.2. Characterization

The dramatic contrasts of functional groups were verified by a Perkin–Elmer Spectrum 2000 FTIR (MNGNA-IR 550, Nicolet, American) in the range of 4,000–400 cm^{-1} using the KBr pellet technique at room temperature. The surface morphologies of samples were characterized by high- and low-vacuum scanning electron microscopy (SEM, JSM-5610LV, Tokyo, Japan), operating at 20 kV. The decomposition properties of chelating resins were measured by thermogravimetric analyzer (TGA, TG209, Netzsch, Germany) at the temperatures ranging 20–700℃ at a scanning rate of 10.0 K min^{-1} under N_2 atmosphere. The specific surface areas were calculated based on BET method, and ASAP 2020 N Physisorption Analyzer (American, Micromeritics) was employed. Atomic adsorption analysis of different metal ions was carried out on a 932B atomic adsorption spectrophotometer (AAS). Nitrogen content of resins was measured by elemental analyzer (Vario EL cube, Elementar, Germany) with analytical precision for C, H, N, S ≤ 0.1%, and O ≤ 0.2%.

2.3. Typical procedures for preparation of 8-HQ-functionalized PGMA resin (HQPGMA)

The typical procedures for preparation of HQPGMA resin was illustrated in Fig. 1. Spherical

PGMA was synthesized according to the method reported elsewhere [29]. Afterward a certain amount of PGMA and DETA were put into a 500-mL three-necked bottle under refluxing. The aminated resin named as ANPGMA was obtained after vacuum drying. It was then mixed with 5-chloromethylation-8-HQ under refluxing in the presence of ethyl alcohol. The pH was kept at 6.0 buffered by $NaHCO_3$. The resulting material HQPGMA resin was purified by extraction with ethyl alcohol for 24 h. Finally, it was processed by vacuum oven until constant weight was recorded at room temperature. The samples obtained were used for FTIR, SEM, and TGA characterization. The surface properties of the resin were determined based on ASAP 2020 N Physisorption Analyzer as well.

2.4. Adsorption capacity toward different metal ions

Adsorption capacity of HQPGMA toward different metal ions was conducted at 25°C for 24 h. Certain amount of resin and certain concentration of metal ion were adequately mixed together. The supernatant was taken out, and the concentration of metal was calculated in light of EDTA titration method. The adsorption capacity was evaluated using the following equation:

$$Q_e = (C_0 - C_e)V/W \quad (1)$$

where Q_e (mmol g^{-1}) is the equilibrium adsorption capacity per unit amount of the adsorbent, C_0 (mmol mL^{-1}) and C_e (mmol mL^{-1}) stand for the initial concentration and equilibrium concentration of Pb(II), respectively, V (mL) is the volume of solution, and W (g) indicates the weight of the HQPGMA resin.

2.5. Adsorption properties of Pb(II)

2.5.1. Effect of pH on adsorption

Effect of pH on adsorption was conducted at 25°C for 24 h. Seven of 100 mg HQPGMA reins, 20 mL 0.02264 mol L^{-1} Pb(II), and 20 mL buffer solution were put into seven iodine flasks in a shaker, respectively. The values of buffer solution were 1.53, 2.55, 3.81,

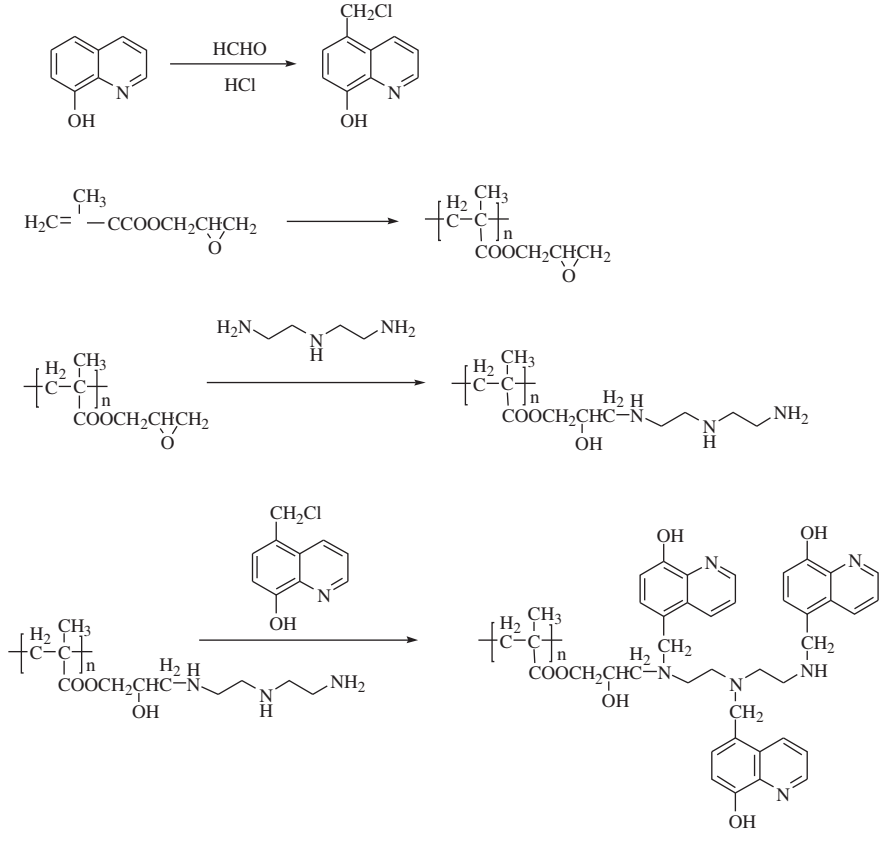

Fig. 1. The typical procedures for synthesis of HQPGMA resin.

4.91, 5.81, 6.45, and 7.03, respectively. The supernatant was taken out, and the concentration of Pb(II) was calculated using EDTA titration method.

2.5.2. Adsorption kinetics

The adsorption kinetics experiments were performed by adding 500 mg HQPGMA resin and 100 mL 0.02264 mol L^{-1} Pb(II) (pH 5.81) into three iodine flasks under different temperatures. A certain volume of solution was withdrawn at intervals from the same iodine flask. The concentration of Pb(II) was calculated by the same EDTA titration method as described above. The following equation was used to calculate the adsorption capacity:

$$Q_n = Q_{n-1} + (C_{n-1} - C_n)V_{n-1}/W \quad (2)$$

where n is the times of sampling, C_{n-1} (mmol mL^{-1}) and C_n (mmol mL^{-1}) represent the concentration of Pb (II) at the $(n-1)$th time and the (n)th time, V_{n-1} (mL) represents the solution volume at the $(n-1)$th time of sampling, Q_{n-1} (mmol g^{-1}) and Q_n (mmol g^{-1}) are the adsorption capacity after the $(n-1)$th time and the (n)th time of sampling, respectively.

2.5.3. Isothermal adsorption

Six of 100 mg HQPGMA resin and various concentrations of Pb(II) (pH 5.81) were put into six iodine flasks, respectively. The adsorption amounts of Pb(II) were obtained after 24 h under the constant temperature. The calculation of concentration of Pb(II) obeyed the above-mentioned way and the adsorption capacity complied with the Eq. (1).

2.5.4. Adsorption selectivity

EDTA titration method cannot be used to determine metal ions concentrations when they are mixed. In this study, AAS is applied to solve this problem. To determine the adsorption selectivity of HQPGMA resin for Pb(II), all the experiments were performed at 25℃ for 24 h. A total of 70 mg HQPGMA resins and 20 mL solution, composed in 18 mL NaAc-HAc buffer solution (pH 5.81), 1 mL Pb(II) (0.1 mol L^{-1}), and 1 mL another metal ion (0.1 mol L^{-1}) solution, were added into three iodine flasks in a shaker. The adsorption capacity was calculated by Eq. (1) as described above.

2.5.5 Desorption performance and of Pb(II)

Effect of elution time and eluent concentrations was determined at 25℃ by adding 1,000 mg dry HQPGMA resin with saturated adsorption and 50 mL hydrochloric solution into four iodine flasks. Concentrations of the eluent varied from 0.2 to 0.8 mol L^{-1}. The supernatant was taken out every 30 min, and the concentration of Pb(II) was determined. In addition, the dynamic desorption was conducted with 0.4 and 0.6 mol L^{-1} hydrochloric solution. In order to test the applicability of this resin for future commercial uses, the process of desorption was performed via wet packing method using 1.8013 g fully swelling HQPGMA resin with saturated adsorption. The desorption amount of Pb(II) was calculated according to Eq. (1).

2.5.6 Regeneration

After dynamic desorption, the resin was separated and washed with distilled water until pH reached 7. Then, the resin was placed in vacuum drying oven at 60℃ until constant weight was recorded at room temperature. Afterward, it was immersed into the Pb(II) solution again for the re-adsorption. To test the reusability of the resin, adsorption–desorption cycles were repeated three times with the same adsorbent.

3. Results and discussion

3.1. Preparation and characterization of HQPGMA resin

The yield of spherical PGMA was 86.92%, and their size was measured at a range of diameter of 0.5–1.7 mm. The epoxy value of PGMA was 3.63 mmol g^{-1} derived by hydrochloric acid–acetone titration method. The yield of ANPGMA resin was 82.26%. The amount of 8-HQ grafting from macromolecular skeleton was 0.635 mmol g^{-1} determined gravimetrically. The purity of HQPGMA was 99.2% after extraction with ethyl alcohol. The copolymer HQPGMA resin was non-water-soluble. The nitrogen contents of ANPGMA and HQPGMA resins determined by element analyzer were 6.38 and 8.66%, respectively. The active site of adsorbent HQPGMA was calculated as 0.71 mmol g^{-1}. Here, FTIR is used to confirm the presence of certain functional group of the modified material, and the results are presented in Fig. 2. Compared with Fig. 2, PGMA and ANPGMA peaks at 845 and 907 cm^{-1} disappeared, which belonged to the stretching vibration of epoxy groups of PGMA. It is demonstrated that amination reaction was proceeded successfully. In contrast to ANPGMA and HQPGMA, three new peaks at 1,462, 1,504, and 1,634 cm^{-1} appeared, which were ascribed to the stretching vibration of benzene group in 8-HQ. The proof mentioned above implied success in the modification of ANPGMA with 8-HQ. The SEM

images of PGMA, ANPGMA, and HQPGMA are presented in Fig. 3. It can be seen from Fig. 3 that the particle size was distributed at 0.12–0.18 mm. Furthermore, the sphere appearances of ANPGMA and HQPGMA were similar to that of PGMA, demonstrating that PGMA possessed excellent mechanical stability and the sphere structure was not destroyed during the modification process. Compared with PGMA, the surface of functionalized derivatives became much rougher, indicating the successful introduction of functional groups onto the surface of PGMA. Percentage weight loss as a function of temperature (up to 800˚C) in thermogravimetric studies for PGMA, ANPGMA, and HQPGMA is shown in Fig. 4. As can be observed, all the materials exhibited two thermogravimetric profiles. The weight loss of PGMA was 5.5% when the temperature reached 150˚C, while weight loss of ANPGMA and HQPGMA reached 9.8 and 12.5% at 90˚C, respectively. Furthermore, more weight loss was observed in comparison with that of PGMA. The phenomena may be attributed to not only the water loss from the consideration of hydroxy in the presence of resins but also chain breakage caused by part of DETA and 8-HQ. While weight loss of PGMA, ANPGMA and HQPGMA were 95.56, 79.68, and 82.21%, respectively, under the temperature of 500˚C, indicating that the modified resins were relatively stable. On the other hand, relatively lower weight loss of ANPGMA, and HQPGMA demonstrated that the graft process was successful. Therefore, the HQPGMA resin could be applied under the temperature of 100˚C. Fig. 5 shows the nitrogen adsorption–desorption isotherm of HQPGMA resin. The isotherm was identified as type IV according to the IUPAC classification which is characterized by the hysteresis loops. The volume adsorbed for isotherm sharply increased at a relative pressure (P/P_0) of approximately 0.8, representing capillary condensation of nitrogen with the uniform mesoporous structure.

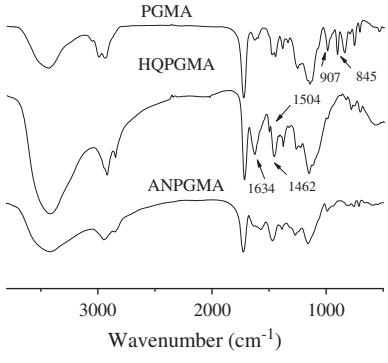

Fig. 2. FTIR spectra of PGMA, ANPGMA and HQPGMA.

The porous structure parameters corresponding parameters of the sample were summarized in Table 1. As can be seen from Table 1, that BET surface area, single point adsorption total pore volume of pores, BJH desorption cumulative volume of pores, and BJH desorption average pore diameter were 425.77 $m^2\ g^{-1}$, 0.48 $cm^3\ g^{-1}$, 0.44 $cm^3\ g^{-1}$, and 4.29 nm, respectively.

3.2. Adsorption capacities of HQPGMA resin for different metal ions

The adsorption capacities of HQPGMA resin were different toward various metal ions, which are listed in Table 2. One of the important influence factors was the absolute electronegativity of metal ions. The stronger the absolute electronegativity of metal ions is, the higher the adsorption amount will reach. In comparison with Pb^{2+}, Cd^{2+}, Cu^{2+}, and Ni^{2+}, the strongest absolute electronegativity was Pb^{2+}. Compared with that of Pb(II), the adsorption capacities of HQPGMA resin for other toxic metal ions were much lower. As a result, Pb(II) was selected to be the target ion.

3.3. Effect of pH on adsorption of HQPGMA resin for Pb(II)

pH is one of the critical parameters in adsorption of metal ions due to the changes of surface charge of the adsorbent and the metal ion chemistry. To investigate the effect of pH on adsorption of HQPGMA resin for Pb(II), experiments were proceeded with a series of pH buffer solution under 25˚C for 24 h. As exhibited in Fig. 6, pH played a key role in adsorption process and the optimal pH was found to be about 5.81. In this experiment, metal precipitation appeared at the range of 7.23–7.53 calculated using lead hydroxide ($Pb(OH)_2$) solubility product at 25˚C. As a result, there was no metal precipitation in the range of pH 3–6. Furthermore, the pH of the solution increased for hydroxy exchange during the adsorption process. The adsorption capacity increased until the highest level, and then decreased. When pH was lower than 5.81, Pb(II) and hydrogen H^+ competed in combination with the active sites of adsorbent due to relatively higher concentration of H^+. Furthermore, the electrostatic repulsion between Pb(II) and the positively charged functional groups may prevent the adsorption of Pb(II) onto the surface of the HQPGMA resin. Therefore, the adsorption of Pb(II) in strong acidic solution was unfavorable. Hydrolyzation of Pb(II) would occur when pH surpassed 5.81, hence decreasing the possibility of Pb(II) incorporation with chelating sites. As a result, the adsorption capacity dropped down.

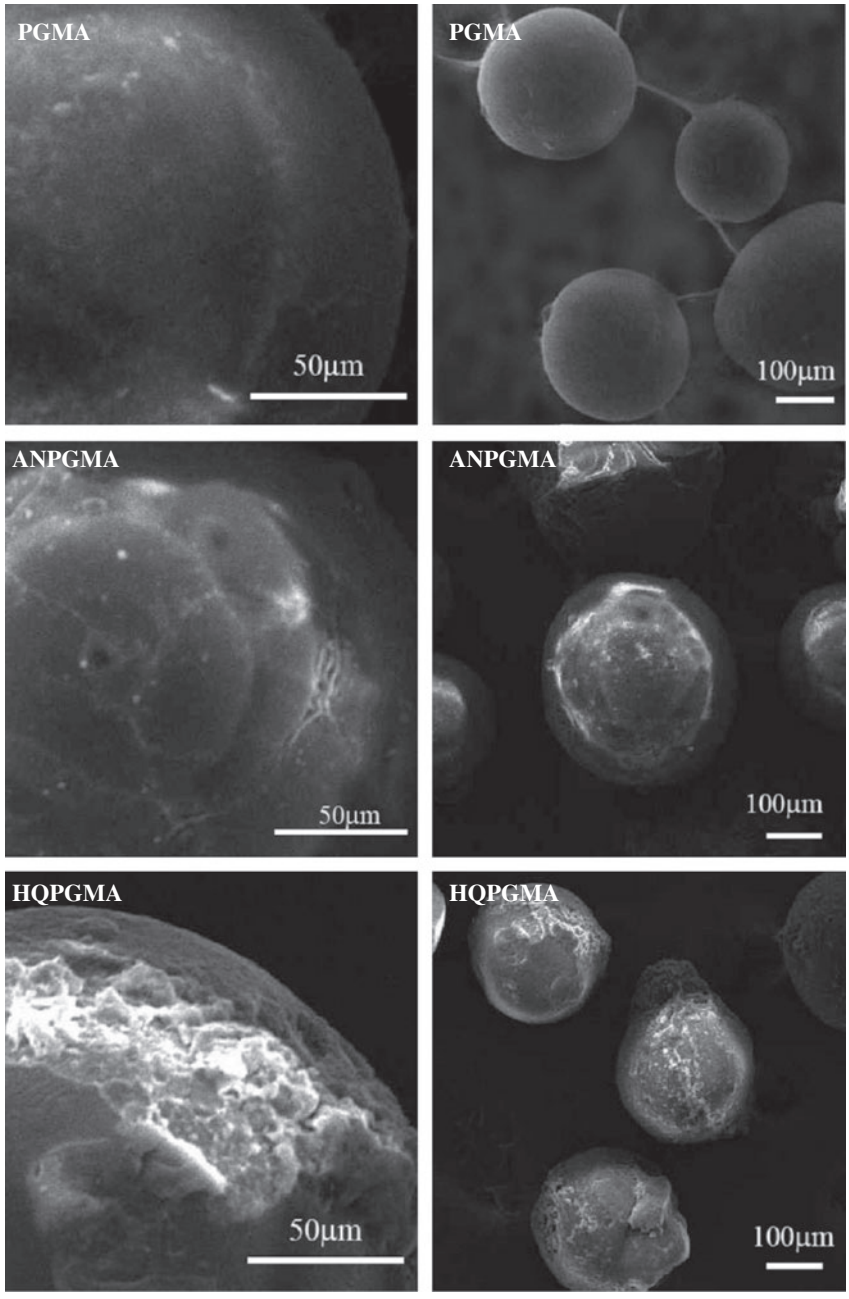

Fig. 3. SEM photographs of PGMA, ANPGMA, HQPGMA.

3.4. Adsorption kinetics

Adsorption kinetics is important in wastewater treatment as it provides valuable insights into the adsorption mechanism, which is important for adsorption efficiency improvement. Adsorption kinetics experiments of Pb(II) under various temperatures are shown in Fig. 7. Two stages can well describe the process of adsorption kinetics. The adsorption speed was relatively higher at the first 600 min due to sufficiently available bonding sites presented by HQPGMA resin. Pb(II) could easily diffuse to combine the bonding sites with the help of mass transfer driving force caused by the concentration gradient. When it reached the second stage, adsorption curve levelled off for equilibrium concentration of Pb(II) at the surface and in the solution at a given temperature. On the other hand, the maximum uptake in this work was 1.38 mmol g^{-1}, much higher than that of Pb(II)

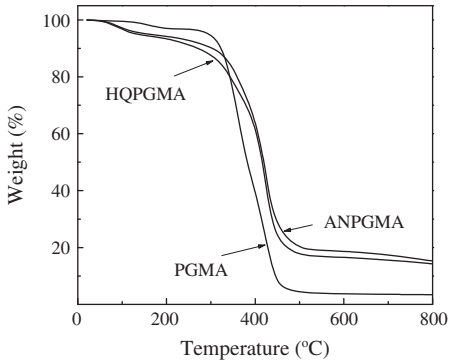

Fig. 4. TGA curves of PGMA, ANPGMA and HQPGMA.

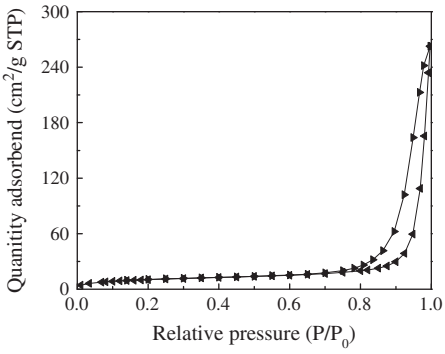

Fig. 5. Nitrogen adsorption-desorption isotherm of HQPGMA resin.

(0.58 mmol g^{-1}) with cross-linked chitosan-poly(aspartic acid) as the adsorbent. Both of them possessed approximately the same equilibrium time [30]. In the other adsorbent named as HQ-PHEMA/SiO_2, in which hydroxyethyl methacrylate (HEMA) was first grafted onto silica gel particles, the adsorption capacity of Pb(II) was as high as 0.3 mmol g^{-1}. As a result, HQPGMA resin synthesized in our research group was a highly efficient adsorbent material [31].

In order to understand the kinetics adsorption mechanism and its potential rate-controlling steps, two diffusion patterns, i.e. film diffusion and particle diffusion, can be applied to describe the adsorption process according to theories put forward by Wang [32] and Boyd [33]. The data were calculated by the following equations presented by Boyd [33] and Reichenberg [34].

$$F = 1 - \frac{6}{\Pi^2}\sum_{n=1}^{\infty}\frac{1}{n^2}\left[\frac{-D_i t \Pi^2 n^2}{r_0^2}\right] \quad (3)$$

$$F = \frac{Q_t}{Q_0} \quad (4)$$

$$B = \frac{\Pi^2 D_i}{r_0^2} \quad (5)$$

wherein Q_t (mmol g^{-1}) and Q_0 (mmol g^{-1}) represent the adsorption capacity at time t and the maximum capacity, respectively; D_i was effective diffusion coefficient of the metal ion; r_0 stands for the radius of adsorbent, supposing that the absorbent was spherical; n, as an integer, defines the infinite series solution.

Table 2
Adsorption capacity of HQPGMA resin for different metal ions

Metal ion	Pb^{2+}	Cd^{2+}	Cu^{2+}	Ni^{2+}
Q_e (mmol g^{-1})	1.375	0.861	0.839	0.165

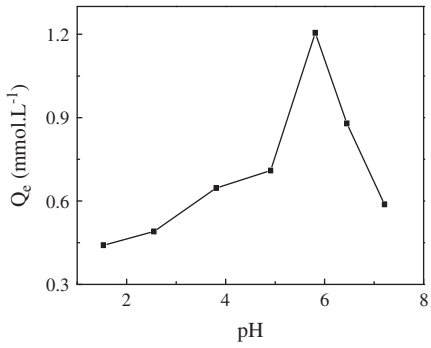

Fig. 6. The effect of pH on the adsorption of Pb(II) onto HQPGMA resin.

Table 1
Parameters of porous structure of HQPGMA resin

BET surface area (m^2 g^{-1})	Single point adsorption total pore volume of pores (cm^3 g^{-1})	BJH desorption cumulative volume of pores (cm^3 g^{-1})[a]	BJH desorption average pore diameter (nm)
425.77	0.48	0.44	4.29

[a]The BJH desorption cumulative volume v of pores between 1.8 and 196 nm diameter.

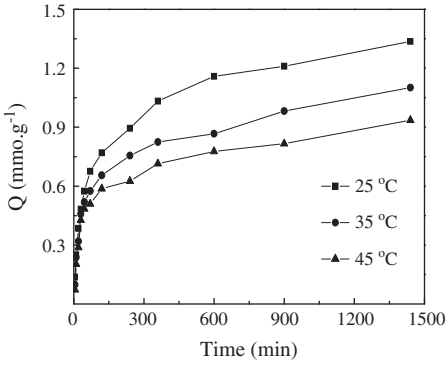

Fig. 7. Adsorption kinetics of Pb(II) onto HQPGMA resin under different temperatures.

B_t was obtained according to the corresponding values of F given by Boyd [33]. If the linearity relationship of B_t vs. t passes through the origin, the rate-controlling step is particle diffusion. Otherwise film diffusion is in charge of absorption process.

As shown in Fig. 8, all the lines showed well linear relationship without passing through the origin, demonstrating that film diffusion was rate-controlling step during the adsorption process. The linear equations and correlation coefficients (R^2) are listed in Table 3.

Pseudo-first-order and pseudo-second-order are the commonly used two models to interpret absorption mechanism [35,36]. Equations are listed as follows:

$$\ln\frac{Q_e - Q_t}{Q_e} = -k_1 t \tag{6}$$

$$\frac{t}{Q_t} = \frac{1}{k_2 Q_e^2} + \frac{t}{Q_e} \tag{7}$$

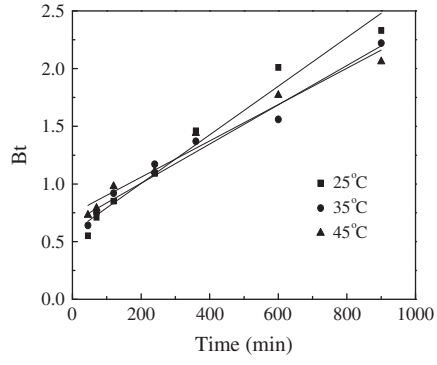

Fig. 8. B_t vs. time plots for HQPGMA resin.

Table 3
The B_t vs. t linear equations and correlation coefficient R^2

T (℃)	Linear equation	R^2
25	$B_t = 0.0211t + 0.5823$	0.9651
35	$B_t = 0.0017t + 0.6694$	0.9675
45	$B_t = 0.0016t + 0.5823$	0.9631

where k_1 (min^{-1}) and k_2 ($g(mmol\ min)^{-1}$) mean the rate constants of pseudo-first-order and pseudo-second-order models, respectively.

In contrast to Figs. 9 and 10, the linearity of t/Q_t vs. t was better than that of $\ln(Q_e - Q_t)$ vs. t, indicating that pseudo-second-order model was more appropriate to describe the absorption kinetics of HQPGMA resin for Pb(II). Values of correlation coefficient (R^2) of pseudo-second-order model, as assessed by Table 4, were much closer to 1, suggesting that pseudo-second-order model is more suitable to describe the adsorption process. It can also be observed that the equilibrium adsorption capacities ($Q_{e(cal)}$) based on pseudo-second-order model were much better in agreement with the experimental data ($Q_{e(exp)}$), further indicating the kinetics adsorption process followed pseudo-second-order model.

3.5. Isothermal adsorption

Adsorption isotherms are of great concern as they provide information about the adsorption capacity and how adsorbate interacts with adsorbent, which are critical in optimizing the application of an adsorbent. To investigate isothermal adsorption of HQPGMA resin for Pb(II) (pH 5.81), experiments were conducted under 25, 35, and 45℃, respectively. It can be seen from Fig. 11 that the adsorption capacity decreased with the temperature rising, indicating that the adsorption process was exothermic. In terms of the same temperature, the adsorption capacity increased with a higher concentration of Pb(II). It may be due to the greater driving force by a higher concentration gradient pressure.

In order to well understand the adsorption mechanism and assess the adsorption characteristics, the isotherms data were analyzed with Langmuir and Freundlich models [37,38]. Langmuir model suggests that adsorption occurs on a homogeneous surface and all the chelating sites are energetically identical. Freundlich model means that adsorption takes place on a heterogeneous surface with adsorption sites having different energies. The linear expression of Langmuir and Freundlich models can be expressed as the following equations:

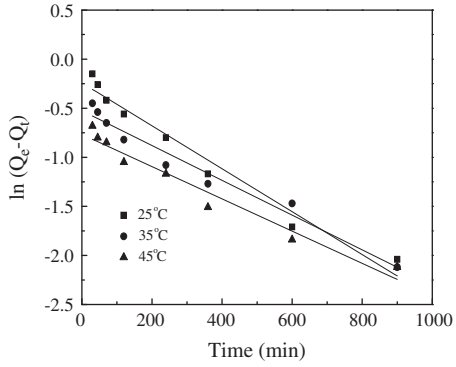

Fig. 9. Pseudo-first-order kinetic plots for adsorption of Pb(II).

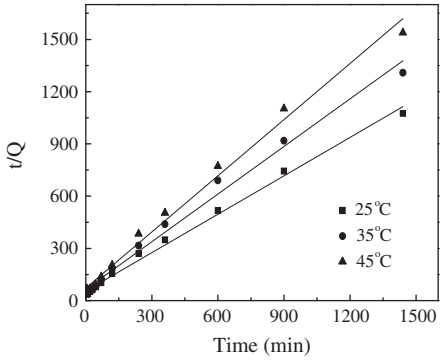

Fig. 10. Pseudo-second-order kinetic plots for adsorption of Pb(II).

$$\frac{C_e}{Q_e} = \frac{C_e}{Q_0} + \frac{1}{Q_0 K_L} \tag{8}$$

$$\ln Q_e = \ln K_F + \frac{\ln C_e}{n} \tag{9}$$

where K_L (mL mmol^{-1}) and K_F (mmol g^{-1}) are the Langmuir and Freundlich constants, respectively, and n is the Freundlich exponent related to adsorption intensity.

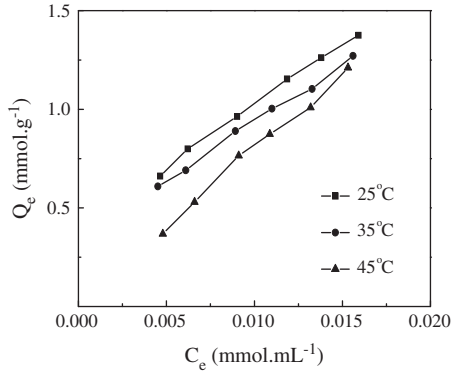

Fig. 11. The adsorption isotherms of Pb(II) onto HQPGMA resin at different temperatures.

In contrast to Figs. 12 and 13, the linearity of Freundlich was much better than that of Langmuir model. The fitting parameters of Freundlich and Langmuir models are presented in Table 5. The correlation coefficients (R^2) obtained from Freundlich model were much higher than those of Langmuir model. Therefore, it can be noted that the adsorption of Pb(II) onto HQPGMA resin can be well fitted by Freundlich model. In other words, the adsorption of Pb(II) onto HQPGMA resin occurred by multilayer adsorption process.

The comparison of q_{max} between HQPGMA and other adsorbents such as natural bentonite and 8-HQ modified magnetic mesoporous carbon is presented in Table 6. The adsorption capacity of HQPGMA was relatively higher than those of alternative adsorbents. This mainly attributed to the structural characteristics of HQPGMA, which is a unique chelating agent because of its high density of nitrogen and oxygen ligands. It can enhance the bonding capacity for Pb(II), which is shown in Fig. 14.

To further understand the adsorption phenomena, the thermodynamic parameters such as Gibbs free energy changes (ΔG), enthalpy change (ΔH), and entropy change (ΔS) were calculated according to the following equations [39]:

Table 4
The maximum adsorption capacities ($Q_{e(exp)}$, $Q_{e(cal)}$) and parameters (k, R^2) of Pseudo-first-order and Pseudo-second-order at different temperatures

T (℃)	$Q_{e(exp)}$ (mmol g^{-1})	Pseudo-first-order kinetics			Pseudo-second-order kinetics		
		k_1 (min^{-1})	$Q_{e(cal)}$ (mmol g^{-1})	R_1^2	k_2 (g mmol^{-1} min^{-1})	$Q_{e(cal)}$ (mmol g^{-1})	R_2^2
25	1.34	−0.00218	0.7843	0.9620	0.7354	1.3600	0.9938
35	1.10	−0.00117	0.5907	0.9675	0.9112	1.0975	0.9894
45	0.94	−0.00164	0.4642	0.9541	1.0742	0.9309	0.9905

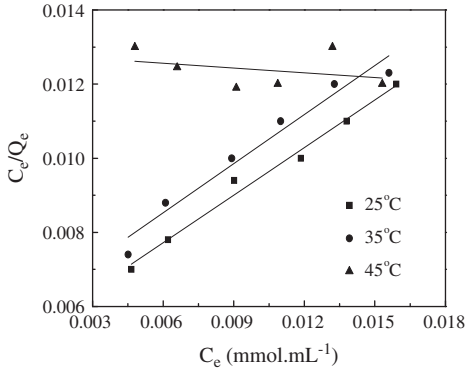

Fig. 12. Langmuir isotherm of HQPGMA resin for Pb(II) at different temperatures.

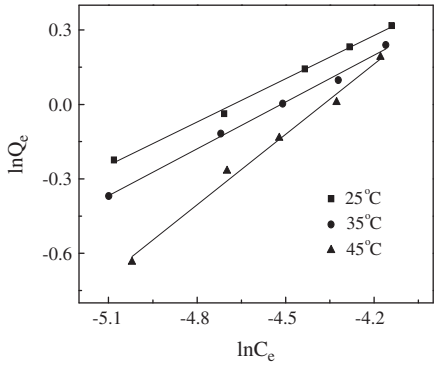

Fig. 13. Freundlich isotherm of HQPGMA resin for Pb(II) at different temperatures.

$$\log K_c = \frac{\Delta S}{2.303R} - \frac{\Delta H}{2.303RT} \quad (10)$$

$$\Delta G = \Delta H - T\Delta S \quad (11)$$

where K_c represents the distribution coefficient that is calculated as the ratio of Pb(II) equilibrium concentration in the adsorbents and aqueous phases, R is the gas constant (8.314 J mol^{-1} K^{-1}), and T (K) is Kelvin temperature. ΔH and ΔS can be obtained from the slope and intercept of the linear plot of $\log K_c$ as a function of $1/T$.

The thermodynamic parameters are listed in Table 7. The negative value of ΔH (−27.16 kJ mol^{-1}) indicates that the adsorption process was exothermic, which was in accord with the behavior of thermodynamics adsorption. As a result, the increase of temperature may inhibit the adsorption of Pb(II). The negative value of ΔS (−49.51 J mol^{-1} K^{-1}) reveals a decrease in the randomness at the solid–solution interface during the adsorption process. The negative values of ΔG (−12.40, −11.66, and −10.18 kJ mol^{-1}) indicate that the adsorption was a spontaneous process. They decreased with the increasing temperature, indicating that the adsorption became more feasible at low temperature. Thus, the thermodynamic reveals the adsorption processes of Pb(II) were spontaneous and could be promoted by decreasing the temperature.

Table 5
Langmuir parameters and Freundlich parameters at different temperatures

	Langmuir parameters			Freundlich parameters		
T (℃)	Q_0 (mmol g^{-1})	K_L	R_L^2	K_F	n	R_F^2
25	2.3363	83.11	0.9841	15.24	1.7172	0.9963
35	2.2654	75.07	0.9544	17.18	1.5879	0.9940
45	−23.1321	−3.37	−0.1077	62.50	1.0574	0.9886

Table 6
Comparison of monolayer maximum adsorption capacities (q_{max}) of some adsorbents for Pb(II) from aqueous solution

Adsorbents	q_{max} (mmol g^{-1})	Refs.
HQPGMA	1.38	This study
Sodium tetraborate-modified Kaolinite clay	0.31	[40]
Natural bentonite	0.41	[41]
Natural and treated bentonite	0.56	[42]
Silica-gel supported PAMAM dendrimers	0.80	[43]
8-HQ modified magnetic mesoporous carbon	1.20	[44]

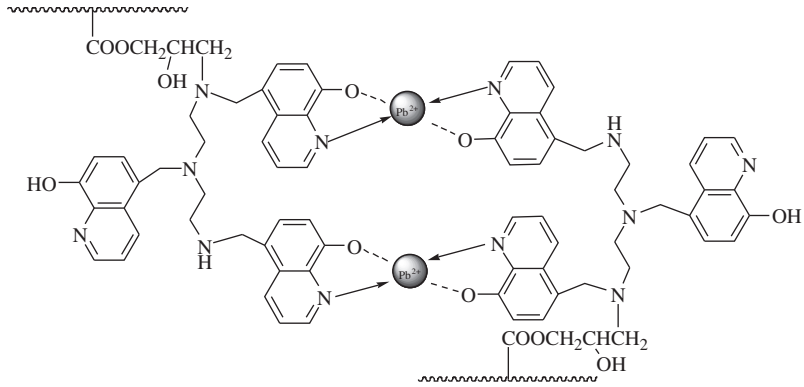

Fig. 14. A suggested bonding mode of HQPGMA resin with favorable binding of Pb(II).

Table 7
Thermodynamic parameters for the adsorption of Pb(II) onto HQPGMA resin at different temperatures

T (K)	ΔG (kJ mol^{-1})	ΔH (kJ mol^{-1})	ΔS (J mol^{-1} K^{-1})
298	−12.40	−27.16	−49.51
313	−11.66		
343	−10.18		

Table 8
Adsorption selectivity of HQPGMA resin

System	Metal ions	Adsorption capacity (mmol g^{-1})	Selective coefficient
Pb^{2+}–Cu^{2+}	Pb^{2+}	0.706	22.77
	Cu^{2+}	0.031	
Pb^{2+}–Ni^{2+}	Pb^{2+}	0.580	20.00
	Ni^{2+}	0.029	
Pb^{2+}–Cd^{2+}	Pb^{2+}	0.4652	22.15
	Cd^{2+}	0.021	

3.6. Adsorption selectivity

A conclusion can be drawn from Table 8 that HQPGMA resin exhibited excellent adsorption capacity toward Pb(II) among different metal ions. As a result, HQPGMA resin was a potential application adsorbent in enrichment recovery of Pb(II) from the mixed metal ions.

3.7. Desorption of HQPGMA resin

The static desorption rate of HQPGMA resin was proceeded in hydrochloric acid solution. As can be seen from Fig. 15, the desorption efficiencies were 70.34, 92.38, 85.91, and 58.10% when concentrations of the eluent were 0.2, 0.4, 0.6, and 0.8 mol L^{-1}, respectively. Our results showed that 0.4 mol L^{-1} hydrochloric acid solution was selected to be the optimal candidate for stripping Pb(II) from HQPGMA resin. Subsequently, 0.4 mol L^{-1} hydrochloric acid solution was used as the eluent in dynamic desorption. As shown in Fig. 16, the desorption amount was stable when desorption efficiency reached 90%. The equilibrium time of desorption was 25 min. These results showed that HQPGMA resin was a potential material due to its excellent adsorption–desorption property.

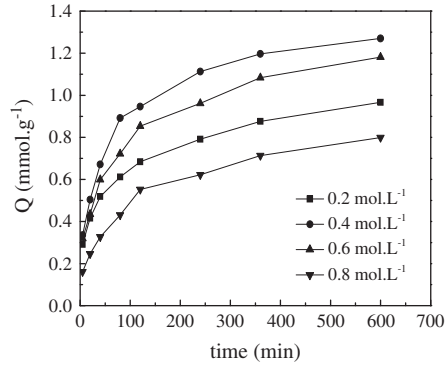

Fig. 15. The desorption curves of HQPGMA resin for Pb(II) with various concentrations of hydrochloric acid solution as eluent.

3.8. Reusability of HQPGMA resin

The reusability of the resin was investigated after three times of adsorption/desorption. As can be seen from Fig. 17, only a minimum decrease in the adsorption efficiency was observed after second and third regeneration. The resin retain Pb(II) uptake of 90.2% after three use cycles. This clearly indicated that

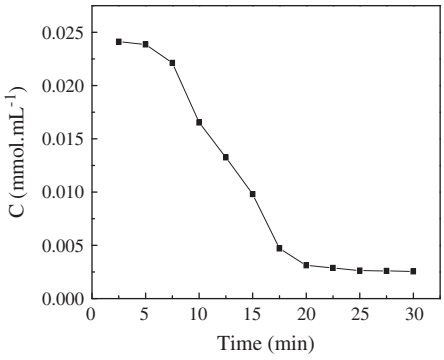

Fig. 16. The dynamic desorption curve of HQPGMA resin for Pb(II) with 0.4 mol L^{-1} hydrochloric acid solution as eluent.

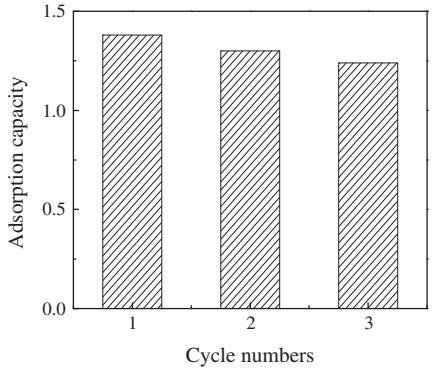

Fig. 17. The regeneration properties of HQPGMA resin.

HQPGMA resin can be used as an effective Pb(II) recovery material with high adsorption capacity and selectivity and a high regeneration property.

4. Conclusion

HQPGMA resin functionalized with 8-HQ was demonstrated to be one promising candidate absorbent for toxic Pb(II). It gained a maximum absorption capacity of 1.38 mmol g^{-1}. Adsorption kinetics was found to follow the pseudo-second-order model with film diffusion as the rate-controlling step. Adsorption isotherms fitted better with Freundlich models. The adsorption process was exothermic. The desorption rate was 92.38% when using 0.4 mol L^{-1} hydrochloric acid solution as eluent. The resin exhibited the same efficiency for adsorption after regeneration for three times. These results suggest that HQPGMA resin that synthesized via "graft from" route is a promising candidate for Pb(II) adsorption from aqueous solution.

Acknowledgments

This study was supported by National Natural Scientific Foundation of China (No. 21171085), Natural Scientific Foundation of Shandong Province (ZR2010BM027, ZR2009BL014), the Program for Scientific Research Innovation Team in Colleges and Universities of Shandong Province, and Wanhua Chemical Group Co., Ltd.

References

[1] M. Sarioglu, S. Akkoyun, T. Bisgin, Inhibition effects of heavy metals (copper, nickel, zinc, lead) on anaerobic sludge, Desalin. Water Treat. 23 (2010) 55–60.
[2] W.S. Wan Ngah, L.C. Teong, M. Hanafiah, Adsorption of dyes and heavy metal ions by chitosan composites: A review, Carbohydr. Polym. 83 (2011) 1446–1456.
[3] D. Kar, P. Sur, S.K. Mandai, T. Saha, R.K. Kole, Assessment of heavy metal pollution in surface water, Int. J. Environ. Sci. Technol. 5 (2008) 119–124.
[4] P.K. Rai, Heavy metal pollution in aquatic ecosystems and its phytoremediation using wetland plants: An ecosustainable approach, Int. J. Phytorem. 10 (2008) 133–160.
[5] C.H. Peng, B.S. Bai, Y.F. Chen, Study on the preparation of Mn-Zn soft magnetic ferrite powders from waste Zn-Mn dry batteries, Waste Manage. 28 (2008) 326–332.
[6] T.Y. Huang, W. Wu, W.W. Li, Identifying the major pollution sources and pollution loading status of Qiputang River in Taihu Lake basin of China, Desalin. Water Treat. 51 (2013) 4736–4743.
[7] Y. Bulut, Z. Tez, Removal of heavy metals from aqueous solution by sawdust adsorption, J. Environ. Sci. 19 (2007) 160–166.
[8] F.J. Garrido-Herrera, I. Daza-Fernández, E. González-Pradas, M. Fernández-Pérez, Lignin-based formulations to prevent pesticides pollution, J. Hazard. Mater. 168 (2009) 220–225.
[9] V.C. Taty-Costodes, H. Fauduet, C. Porte, A. Delacroix, Removal of Cd(II) and Pb(II) ions, from aqueous solutions, by adsorption onto sawdust of *Pinus sylvestris*, J. Hazard. Mater. 105 (2003) 121–142.
[10] J.S. Al-Jariri, F. Khalili, Adsorption of Zn(II), Pb(II), Cr (III) and Mn(II) from water by Jordanian bentonite, Desalin. Water Treat. 21 (2010) 308–322.
[11] M. Zhou, Q. Dai, L. Lei, C.A. Ma, D. Wang, Long life modified lead dioxide anode for organic wastewater treatment: Electrochemical characteristics and degradation mechanism, Environ. Sci. Technol. 39 (2005) 363–370.
[12] A.G. Vlyssides, M. Loizidou, P.K. Karlis, A.A. Zorpas, D. Papaioannou, Electrochemical oxidation of a textile dye wastewater using a Pt/Ti electrode, J. Hazard. Mater. 70 (1999) 41–52.
[13] A. Dąbrowski, Z. Hubicki, P. Podkościelny, E. Robens, Selective removal of the heavy metal ions from waters and industrial wastewaters by ion-exchange method, Chemosphere 56 (2004) 91–106.

[14] V.K. Gupta, A. Mittal, R. Jain, M. Mathur, S. Sikarwar, Adsorption of Safranin-T from wastewater using waste materials-activated carbon and activated rice husks, J. Colloid Interface Sci. 303 (2006) 80–86.
[15] M.A. Shannon, P.W. Bohn, M. Elimelech, J.G. Georgiadis, B.J. Mariñas, A.M. Mayes, Science and technology for water purification in the coming decades, Nature 452 (2008) 301–310.
[16] C. Lu, H. Chiu, Adsorption of zinc(II) from water with purified carbon nanotubes, Chem. Eng. Sci. 61 (2006) 1138–1145.
[17] Y. Xu, Z. Hao, H. Chen, J. Sun, D. Wang, Preparation of polyacrylonitrile initiated by modified corn starch and adsorption for mercury after modification, Ind. Eng. Chem. Res. 53 (2014) 4871–4877.
[18] S. Babel, T.A. Kurniawan, Low-cost adsorbents for heavy metals uptake from contaminated water: A review, J. Hazard. Mater. 97 (2003) 219–243.
[19] L. Mercier, T.J. Pinnavaia, Heavy metal ion adsorbents formed by the grafting of a thiol functionality to mesoporous silica molecular sieves: Factors affecting Hg(II) uptake, Environ. Sci. Technol. 32 (1998) 2749–2754.
[20] V.K. Gupta, A. Mittal, R. Jain, M. Mathur, S. Sikarwar, Adsorption of Safranin-T from wastewater using waste materials-activated carbon and activated rice husks, J. Colloid Interface Sci. 303 (2006) 80–86.
[21] O. Karnitz Jr., L. Gurgel, J. de Melo, V.R. Botaro, T. Melo, R.P. de Freitas Gil, L.F. Gil, Adsorption of heavy metal ion from aqueous single metal solution by chemically modified sugarcane bagasse, Bioresour. Technol. 98 (2007) 1291–1297.
[22] H. Kaşgöz, S. Özgümüş, M. Orbay, Modified polyacrylamide hydrogels and their application in removal of heavy metal ions, Polymer 44 (2003) 1785–1793.
[23] R. Celis, M.C. HermosÍn, J. Cornejo, Heavy metal adsorption by functionalized clays, Environ. Sci. Technol. 34 (2000) 4593–4599.
[24] A. Lezzi, S. Cobianco, A. Roggero, Synthesis of thiol chelating resins and their adsorption properties toward heavy metal ions, J. Polym. Sci. Part A: Polym. Chem. 32 (1994) 1877–1883.
[25] C.N. Fredd, H.S. Fogler, The influence of chelating agents on the kinetics of calcite dissolution, J. Colloid Interface Sci. 204 (1998) 187–197.
[26] S.E. Bailey, T.J. Olin, R.M. Bricka, D.D. Adrian, A review of potentially low-cost sorbents for heavy metals, Water Res. 33 (1999) 2469–2479.
[27] P. Liu, T. Wang, Adsorption properties of hyperbranched aliphatic polyester grafted attapulgite towards heavy metal ions, J. Hazard. Mater. 149 (2007) 75–79.
[28] S.A. Kosa, G. Al-Zhrani, M. Abdel Salam, Removal of heavy metals from aqueous solutions by multi-walled carbon nanotubes modified with 8-hydroxyquinoline, Chem. Eng. J. 181–182 (2012) 159–168.
[29] R.E. Sturgeon, S.S. Berman, S.N. Willie, J. Desaulniers, Preconcentration of trace elements from seawater with silica-immobilized 8-hydroxyquinoline, Anal. Chem. 53 (1981) 2337–2340.
[30] X.J. Chen, J.C. Cai, Z.H. Zhang, L.J. Liu, G.L. Yang, Investigation of removal of Pb(II) and Hg(II) by a novel cross-linked chitosan-poly(aspartic acid) chelating resin containing disulfide bond, Colloid Polym. Sci. 292 (2014) 2157–2172.
[31] Y. Li, B. Gao, X. Fang, Preparation of 8-hydroxyquinoline-type composite chelating material HQ-PHEMA /SiO_2 and its adsorption behavior for heavy metal ions, J. Chem. Technol. Biotechnol. 88 (2013) 1459–1467.
[32] G.E. Boyd, A.W. Adamson, L.S. Myers, The exchange adsorption of ions from aqueous solution by organic zeolites II. Kinetics, J. Am. Chem. Soc. 69 (1947) 2836–2848.
[33] D. Reichenberg, Properties of ion-exchange resins in relation to their structure. III. Kinetics of exchange, J. Am. Chem. Soc. 75 (1953) 589–597.
[34] F. Helfferich, Ion-Exchange, McGraw-Hill, New York, NY, 1962.
[35] R.J. Qu, Y.Z. Niu, J.C.M. Liu, C.M. Sun, Y. Zhang, H. Chen, C.N. Ji, Adsorption and desorption behaviors of Pd(II) on silica-gel functionalized with ester- and amino-terminated dendrimer-like polyamidoamine polymers, React. Funct. Polym. 68 (2008) 1272–1280.
[36] D.A. Fungaro, M. Bruno, L.C. Grosche, Adsorption and kinetic studies of methylene blue on zeolite synthesized from fly ash, Desalin. Water Treat. 2 (2009) 231–239.
[37] M.M. Abd, A.M. El-Latif, Ibrahim, Adsorption, kinetic and equilibrium studies on removal of basic dye from aqueous solutions using hydrolyzed oak sawdust, Desalin. Water Treat. 6 (2009) 252–268.
[38] L. Zhang, S. Hong, J. He, F. Gan, Y.S. Ho, Adsorption characteristic studies of phosphorus onto laterite, Desalin. Water Treat. 25 (2011) 98–105.
[39] Y. Niu, R. Qu, H. Chen, L. Mu, X. Liu, T. Wang, Y. Zhang, C. Sun, Synthesis of silica gel supported salicylaldehyde modified PAMAM dendrimers for the effective removal of Hg(II) from aqueous solution, J. Hazard. Mater. 278 (2014) 267–278.
[40] E.I. Unuabonah, K.O. Adebowale, B.I. Olu-Owolabi, L.Z. Yang, L.X. Kong, Adsorption of Pb (II) and Cd (II) from aqueous solutions onto sodium tetraborate-modified Kaolinite clay: Equilibrium and thermodynamic studies, Hydrometallurgy 93 (2008) 1–9.
[41] B. Anna, M. Kleopas, S. Constantine, F. Anestis, B. Maria, Adsorption of Cd(II), Cu(II), Ni(II) and Pb(II) onto natural bentonite: Study in mono-and multi-metal systems, Environ. Earth Sci. 73 (2015) 5435–5444.
[42] J.A. Hefne1, W.K. Mekhemer, N.M. Alandis, O.A. Aldayel, T. Alajyan, Kinetic and thermodynamic study of the adsorption of Pb(II) from aqueous solution to the natural and treated bentonite, Int. J. Phys. Sci. 3 (2008) 281–288.
[43] Y.Z. Niu, R.J. Qu, C.M. Sun, C.H. Wang, H. Chen, C.N. Ji, Y. Zhang, X. Shao, F.L. Bu, Adsorption of Pb (II) from aqueous solution by silica-gel supported hyperbranched polyamidoamine dendrimers, J. Hazard. Mater. 244–245 (2013) 276–286.
[44] W. Guo, X. Meng, Y. Liu, L. Ni, Z. Hu, R. Chen, M.J. Meng, Y. Wang, J. Han, M. Luo, Synthesis and application of 8-hydroxyquinoline modified magnetic mesoporous carbon for adsorption of multivariate metal ions from aqueous solutions, J. Ind. Eng. Chem. 21 (2015) 340–349.